

Phase derived frequency shift mapping and DTI of white matter regions at 3T

G. E. Hagberg¹, A. Cherubini¹, U. Sabatini¹, and C. Caltagirone¹
¹Santa Lucia Scientific Foundation, Rome, Italy

Introduction

MRI applications based on the phase signal yield a gain in contrast-to-noise between white and gray matter [1], that depends on several factors like fiber orientation with respect to B_0 , slice orientation used for GRE (gradient recalled echo) MRI and type of post-processing used for gradient background removal [e.g. 2]. In the present study we explored the frequency shift (FS) maps derived from the linear phase accrual at six echo times in automatically parcellated white matter regions [3]. We used four methods for gradient background removal and compared the linear fits for the frequency shifts with DTI- derived parameters (fractional anisotropy, FA and mean diffusivity, MD) and $R2^*$ relaxometry values.

Materials and methods

Four out of a total of 30 subjects (17 women, 13 men; 37.4 +/- 14.0 years) who volunteered to participate in the study approved by the local ethics review board were fully evaluated in MNI standard brain space. The MRI scans (3T Allegra, Siemens) included anatomic T1 weighted 3D modified driven equilibrium Fourier transform scans (TE/TR: 2.4ms/7.92ms, angle:15°, voxel: 1x1x1mm³), DTI scans that were repeated three times and included 30 isotropically distributed orientations for the diffusion-sensitizing gradients and b-values of 1000 s/mm² and six b₀ images (TE: 89 ms, TR: 8.5 s, bandwidth(BW) 2126 Hz/pixel, 80 transverse slices, voxel: 1.8x1.8x1.8mm³), and co-localized GRE MRI that was performed at 6 echo times (6, 12, 20, 30, 45, 60 ms) using a segmented EPI read-out train (TR: 5s, BW: 1116 Hz/pixel else same as DTI) and GRE field mapping (TE: 10/12.46ms, voxel: 3x3x3 mm³). The orientation of the 2D slices was along the AC-PC line. Post processing (FSL 4.1 and in-house Matlab v. 7.4 software) of DTI and relaxometry data included: distortion correction of the DTI scans, tensor fitting, calculation of FA and MD; motion correction, realignment and smoothing of the GRE-EPI magnitude data prior to non-linear fitting of $R2^*$ and non-linear image registration to the MNI brain space (Fig2). The phase data was pre-processed by four methods (see Fig1): **A**) Gaussian homodyne k-space filter (5mm FWHM); **B**) cubic spline fitting of the magnitude k-space values (tolerance 1000); **C**) phase unwrapping and cubic spline fitting of the image phase with tolerance 1/1000; **D**) phase unwrapping and 8th order polynomial fitting of the image phase. Linear least-squares regression was performed but gradient values were only retained for pixels with a statistically significant fit ($p < 0.05$). After motion correction, non-linear image registration of the frequency shift maps were performed and averaged across subjects. The JHU-ICBM template was used for automatic WM parcellation of 45 structures (all except Fornix areas).

Results and discussion

Phase pre-processing lead to differences in terms of spatial contiguity (Gaussian and image spline were superior, with limited drop-out in cerebellum and close to the frontal sinuses) and range of values (polynomial and image spline had the greatest range: ±2Hz,

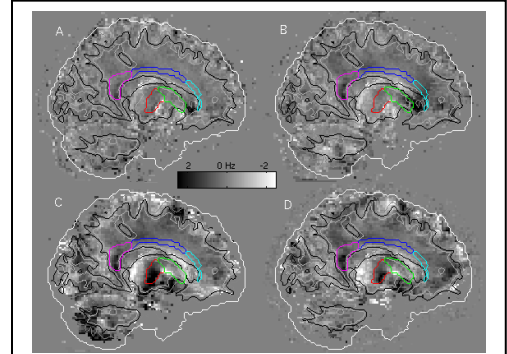


Fig1: Average frequency shift maps after 4 phase pre-processing methods, $x=18$ mm. Contours indicate brain outline, white matter (probability: 0.1, 0.5 and 0.9), commissural fibers, ALIC and PLIC

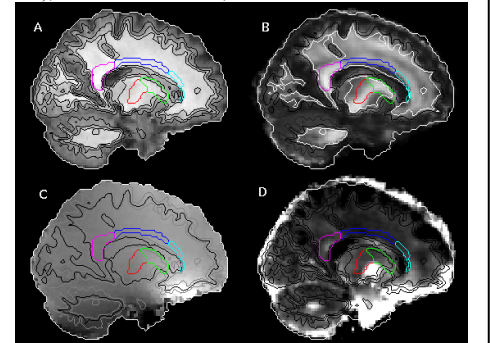


Fig2: A. T1, B. Fractional Anisotropy, C. Fieldmap ±200 Hz, D. $R2^*$ with range: 15-35 s⁻¹

The phase data was pre-processed by four methods (see Fig1): **A**) Gaussian homodyne k-space filter (5mm FWHM); **B**) cubic spline fitting of the magnitude k-space values (tolerance 1000); **C**) phase unwrapping and cubic spline fitting of the image phase with tolerance 1/1000; **D**) phase unwrapping and 8th order polynomial fitting of the image phase. Linear least-squares regression was performed but gradient values were only retained for pixels with a statistically significant fit ($p < 0.05$). After motion correction, non-linear image registration of the frequency shift maps were performed and averaged across subjects. The JHU-ICBM template was used for automatic WM parcellation of 45 structures (all except Fornix areas).

Results and discussion

Phase pre-processing lead to differences in terms of spatial contiguity (Gaussian and image spline were superior, with limited drop-out in cerebellum and close to the frontal sinuses) and range of values (polynomial and image spline had the greatest range: ±2Hz,

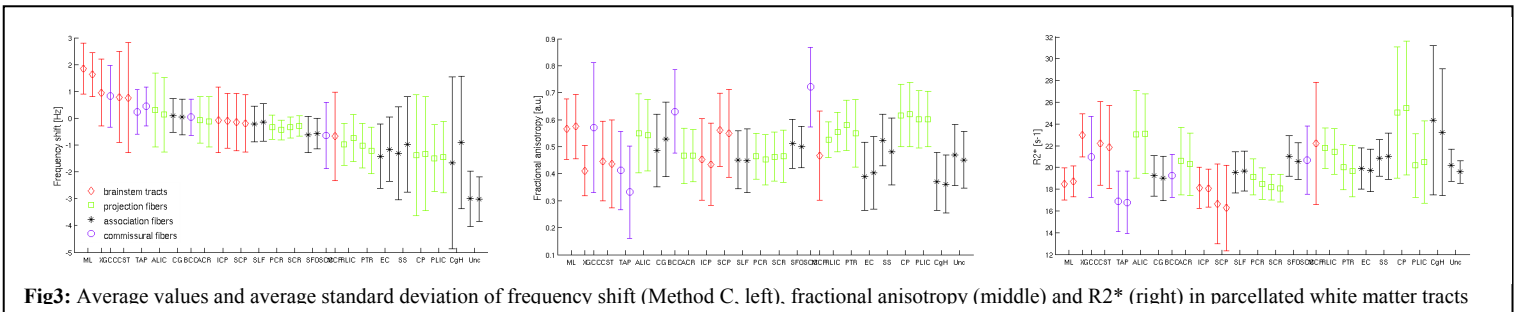


Fig3: Average values and average standard deviation of frequency shift (Method C. left), fractional anisotropy (middle) and $R2^*$ (right) in parcellated white matter tracts

Gaussian filtering the smallest: ±0.5Hz). Comparison of values in different WM regions indicated that frequency shift maps could yield additional and qualitatively different information. The rank order was significantly different between FS, FA, $R2^*$ and MD (Fig3). The combined informational content depends both on fiber orientation and myelin density. In the commissural fibers, FS and MD values decreased from the anterior to the posterior structures while FA increased and $T2^*$ was greatest in the callosal body. The anterior and posterior limbs of the internal capsule were not different in FA or MD, while the FS decreased and the $R2^*$ increased.

[1] Duyn J, et al., 2007. PNAS, 104:11796-11801; [2] Schäfer et al., 2009. NI 48:26; [3] Mori et al., 2008. NI 40:570